

## Effects to System Performance of Different PWM Techniques in Field Oriented Speed Control with back-to-back Converter of PMSG

<sup>1</sup>Naim Suleyman Ting(0000-0003-3743-0824), <sup>2</sup>Yakup Sahin(0000-0002-2787-7115)

<sup>1</sup>Department of Electrical Electronics Engineering, Engineering Faculty of Erzincan Binali Yildirim University, 24100, Erzincan, Turkey

nsuleyman@erzincan.edu.tr

<sup>2</sup>Department of Electrical Electronics Engineering, Engineering Faculty of Bitlis Eren University, 13000, Bitlis, Turkey  
ysahin@beu.edu.tr

Received Date: 13.06.2017 Accepted Date: 31.05.2018

### Abstract

In this paper, the performance of space vector pulse width modulation (SVPWM), sinusoidal pulse width modulation (SPWM) and hysteresis current control (HCC) techniques used in speed control with back to back converter of permanent magnet synchronous generator (PMSG) used in wind turbines are comparatively analyzed. The comparative analysis includes dynamic response, total harmonic distortion (THD), torque ripple and current ripple. Furthermore, SVPWM and SPWM are compared in terms of the using DC link voltage. Analysis of system is realized with MATLAB/Simulink program. PMSG used in simulations is surface mounted, bipolar and its power is 1.8 kW. Also, the energy of PMSG is transferred to grid with Field Oriented Control (FOC). According to analysis results, it has been observed that SVPWM generally has more effective results than both HCC and SPWM control techniques. Finally, it is observed that SVPWM can produce about 15 percent higher than SPWM in output voltage.

**Keywords:** Field oriented control, motor control, back to back converter, space vector pulse width modulation, hysteresis control.

### 1. INTRODUCTION

The utilization of renewable energy sources is becoming increasingly important in terms of energy efficiency in recent years. Wind energy is one of the renewable energy sources. The wind turbines are designed to convert the wind energy to electrical energy over the world. There is an electric machine operated as generator for making conversion to electricity energy from mechanical energy in the structure of wind turbine. There are two types of commonly used generator which double fed induction generator (DFIG) and permanent magnet synchronous generator (PMSG) [1, 2]. PMSG offers better performance due to higher efficiency and less maintenance because it does not have rotor current.

Furthermore, PMSG can be used without a gearbox, which implies a reduction of the weight of the nacelle and reduction of costs [3-16].

The main advantage of PMSG compared to electrical excited synchronous generators is that PMSG does not require any external excitation current. This feature allows to simplify the rotor structure and use a smaller pole pitch. So, the machines can be designed to rotate at rated speeds of 20–100 r/min with multiple poles, depending on the generator rated power [1]-[4].

Field Oriented Control (FOC) is used for energy transmission to grid from generator. This energy

\*Corresponding Author: <sup>1</sup>Department of Electrical Electronics Engineering, Engineering Faculty of Erzincan Binali Yildirim University, 24100, Erzincan, Turkey, nsuleyman@erzincan.edu.tr



rotor to produce the air gap magnetic field instead of using electromagnets. The model of PMSG without damper winding has been developed on rotor reference frame using the following assumptions:

1. Saturation is neglected.
2. The induced EMF is sinusoidal.
3. Eddy currents and hysteresis losses are negligible.
4. There are no field current dynamics [6].

The PMSG dynamic equations are expressed in the d-q reference frame. The voltage equations are given by [1] and flux linkage is given by:

$$\varphi_{sd} = L_d \cdot i_{sd} + \varphi_{sq} = L_q \cdot i_{sq} \quad (1)$$

$$V_{sd} = R_s \cdot i_{sd} + \frac{d\varphi_{sd}}{dt} - \omega_e \cdot \varphi_{sq}$$

$$V_{sq} = R_s \cdot i_{sq} + \frac{d\varphi_{sq}}{dt} - \omega_e \cdot \varphi_{sd} \quad (2)$$

$$P_e = \frac{3}{2} (V_{sd} \cdot i_{sd} + V_{sq} \cdot i_{sq}) \quad (3)$$

Substituting eq (1) in (2) and eq. (2) in (3):

$$P_e = \frac{3}{2} (R_s \cdot i_{sd}^2 + R_s \cdot i_{sq}^2) + \frac{3}{2} \left( L_d \frac{d i_{sd}^2}{dt} + L_q \frac{d i_{sq}^2}{dt} \right) + \frac{3}{2} (\omega_e \cdot i_q \cdot i_d (L_d - L_q) + \omega_e \cdot \phi_m \cdot i_q) \quad (4)$$

In here,  $\phi_m$  is permanent magnet flux,  $\omega_e$  is electrical speed. The first term refers to the power loss in conductors; the second term refers to ratio variation with time of stored energy in magnetic field and finally, the third term refers to energy conversion. The third term also is equal electromagnetic torque because motor shaft power is equal electromechanical power [7].

According to this information, we can use only the third term to calculate electromagnetic torque:

$$T_e = \frac{3}{2} p_p (i_q \cdot i_d (L_d - L_q) + \phi_m \cdot i_q) \quad (5)$$

In this study, since surface mounted PMSG is used, d-axis and q-axis inductances are equal each other. Finally, for PMSG used in this study, electromagnetic torque is shown eq (6):

$$T_e = \frac{3}{2} p_p \cdot \phi_m \cdot i_q \quad (6)$$

## 4. CONTROL TECHNIQUES

The control technique used to obtain the switching signals is fairly important in terms of applicability and productivity. If there is not a good control system, a large part of the generated power is wasted. In this study, it is compared to impact to system performance of SVPWM, SPWM and HCC control techniques.

### 4.1 Space Vector Pulse Width Modulation (SVPWM)

SVPWM is a digital modulation technique used in power converter for switching of semiconductor devices. This technique purposes to minimize switching losses and obtain desired output current or voltage with minimum THD. This control technique's advantages are:

- The less switching power loss due to suitable number of switching compared to HCC.
- More DC bus utilization than SPWM
- Low harmonic content in output current with proper switching pattern selection [8].

SVPWM is basically based to be defined as separate space vectors of every switching situation in inverter. There are eight switching situation in there phase inverter. As shown in Fig. 3, according as these switching situations, it consists of six active vectors and two zero vectors. Then, it is calculated phase and interphase voltages of every switching situation as Fig. 3. Also, these voltage values are shown in Table I.

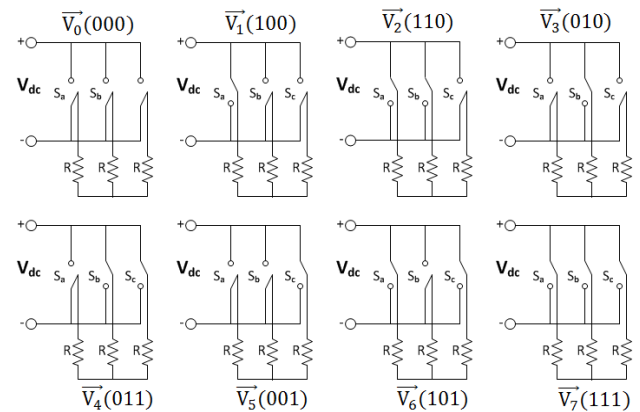


**Fig. 3.** The switching situations of a three phase inverter

The basic principle of SVPWM is to supply a reference voltage vector which approximates as closely as possible to the ideal voltage vector by using eight separate voltage vectors produced by inverter. Finally, it is obtained a reference voltage vector rotated in a hexagonal that created by six active vectors and zero vectors. As shown in Fig. 4, it is consist of six sections in hexagonal. In every section, two active vectors and a zero vector is switched and  $\vec{V}_{ref}$  is produced.

**Table 1.** Phase and interphase voltages according as switching situations

S <sub>a</sub>	S <sub>b</sub>	S <sub>c</sub>	V <sub>a</sub>	V <sub>b</sub>	V <sub>c</sub>	V <sub>ab</sub>	V <sub>bc</sub>	V <sub>ca</sub>
0	0	0	0	0	0	0	0	0
1	0	0	(2/3).V <sub>dc</sub>	(-1/3).V <sub>dc</sub>	(-1/3).V <sub>dc</sub>	V <sub>dc</sub>	0	-V <sub>dc</sub>
1	1	0	(1/3).V <sub>dc</sub>	(1/3).V <sub>dc</sub>	(-2/3).V <sub>dc</sub>	0	V <sub>dc</sub>	-V <sub>dc</sub>
0	1	0	(-1/3).V <sub>dc</sub>	(2/3).V <sub>dc</sub>	(-1/3).V <sub>dc</sub>	-V <sub>dc</sub>	V <sub>dc</sub>	0
0	1	1	(-2/3).V <sub>dc</sub>	(1/3).V <sub>dc</sub>	(1/3).V <sub>dc</sub>	-V <sub>dc</sub>	0	V <sub>dc</sub>
0	0	1	(-1/3).V <sub>dc</sub>	(-1/3).V <sub>dc</sub>	(2/3).V <sub>dc</sub>	0	-V <sub>dc</sub>	V <sub>dc</sub>
1	0	1	(1/3).V <sub>dc</sub>	(-2/3).V <sub>dc</sub>	(1/3).V <sub>dc</sub>	V <sub>dc</sub>	-V <sub>dc</sub>	0
1	1	1	0	0	0	0	0	0

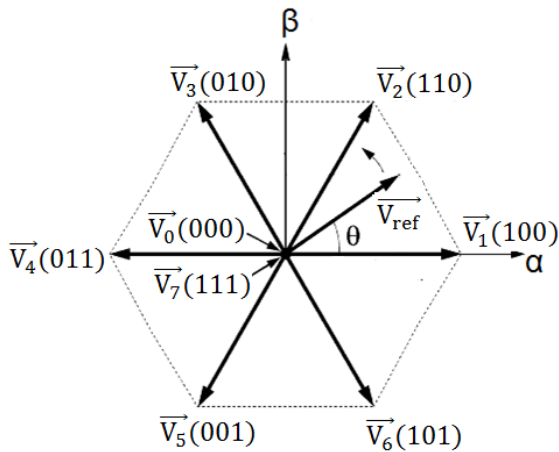


**Fig. 4.** Rotated reference vector in hexagonal

By looking to Fig. 4, it can be obtained the following equations:

$$\vec{V}_{ref} = V_{\alpha} + jV_{\beta} \quad (7)$$

$$V_{ref} = \sqrt{V_{\alpha}^2 + V_{\beta}^2} \quad (8)$$

$$\theta = \tan^{-1} \left( \frac{V_{\beta}}{V_{\alpha}} \right) \quad (9)$$

By using Clarke transformation, it can be written to  $\vec{V}_{ref}$  in three phase axis frame.

$$\vec{V}_{ref} = \frac{2}{3} (V_a \cdot e^{j0} + V_b \cdot e^{j\frac{2\pi}{3}} + V_c \cdot e^{j\frac{4\pi}{3}}) \quad (10)$$

It can be calculated  $\vec{V}_{ref}$  in every section if it is written to inside equation (8)  $V_{abc}$  values. And this reference voltage is expressed a general equation:

$$\vec{V}_k = \frac{2}{3} (V_{dc} \cdot e^{j\frac{(k-1)\pi}{3}}) \quad k=1, 2, 3, 4, 5, 6 \quad (11)$$

Then, it can be obtained the switching signals in four steps:

Step 1: The section where reference voltage is determined.

Step 2: The switching durations ( $T_a$ ,  $T_b$  and  $T_0$ ) are calculated.

Step 3: Control voltages ( $S_1$ ,  $S_3$  ve  $S_5$ ) determining according as optimal switching sequence are calculated.

Step 4: Control voltages ( $S_1$ ,  $S_3$  ve  $S_5$ ) and carrier triangular signal are compared and so, the switching signals are obtained.

#### 4.1.1 Determination of Sections

As shown in Fig. 4, there is a difference of 60 degrees between the vectors. For example, if it is  $0 < \theta < 60^\circ$ ,  $\vec{V}_{ref}$  is first section. Therefore, to know what  $\vec{V}_{ref}$  is in the section  $\theta$  should be calculated.

In eq. (9), the functions as ‘arctan’ and ‘square’ root need to calculate  $\theta$ . But these functions slow down the operating speed of Digital Signal Processor (DSP). Therefore in this paper, it is found in a different way since experimental studies were also considered to be made. The algorithm needed to determinate sections is shown in Fig. 5.

The following equations are given with regard to the algorithm.

$$x = \sqrt{3V_{\alpha}} \quad (12)$$

$$y = -V_\beta \quad (13)$$

$$z = -x \quad (14)$$

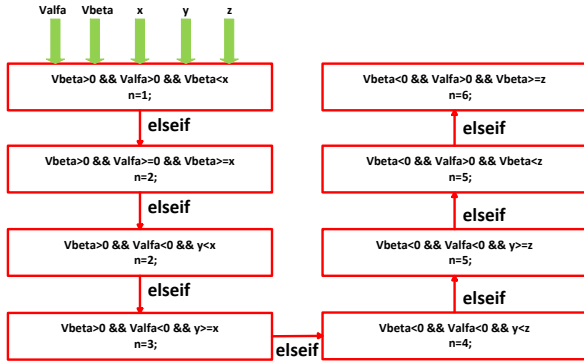


Fig. 5. The algorithm developed to determine the sections

### 4.1.2 Determination of Sections

After the section of  $\vec{V}_{ref}$  is determined by looking Fig. 5, the implementation durations of active vectors in the relevant section can be calculated. For example; in order that  $\vec{V}_{ref}$  is in the first section,  $\vec{V}_1$  should be applied until  $T_a$  time;  $\vec{V}_2$  should be applied until  $T_b$  time;  $\vec{V}_0$  and  $\vec{V}_7$  should be applied until  $T_o$  time. The sum of these three times is equal to a switching period ( $T_s$ ).

According as Fig. 6, it can be written the following equation:

$$\vec{V}_{ref} \cdot T_s = \vec{V}_1 \cdot T_a + \vec{V}_2 \cdot T_b + \vec{V}_0 \cdot \frac{T_o}{2} + \vec{V}_7 \cdot \frac{T_o}{2} \quad (15)$$

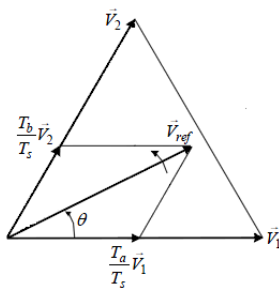


Fig. 6. The switching times in the first section

Substituting eq. (11) in (19) for each vector in the

first section:

$$T_a = m_b \cdot V_a - 0.5m_a \cdot V_\beta \quad (16)$$

$$T_b = m_a \cdot V_\beta \quad (17)$$

In here,  $m_a = \sqrt{3} \frac{T_s}{V_{dc}}$ ,  $m_b = \frac{3}{2} \frac{T_s}{V_{dc}}$

Similar operations are performed also for other sections and times are calculated. These calculations are shown in Fig. 8.

### 4.1.3 Determination of Reference Control Voltages

The most important factor is to ensure the minimum switching loss while reference control voltages are determined. So, the most suitable switching sequence for each section is determined and thereby it is provided minimum switching power loss and better harmonic performance. The most suitable switching is only possible when just one switch is transmission or cutting in each switching period.

Active vectors and zero vectors are  $\vec{V}_0$  and  $\vec{V}_7$  in the first section. And just one switch is active in each switching period as seen from Fig. 7. Therefore, the minimum switching loss is provided with minimum switching number. The most suitable switching sequence for the first section is shown in Fig. 7.

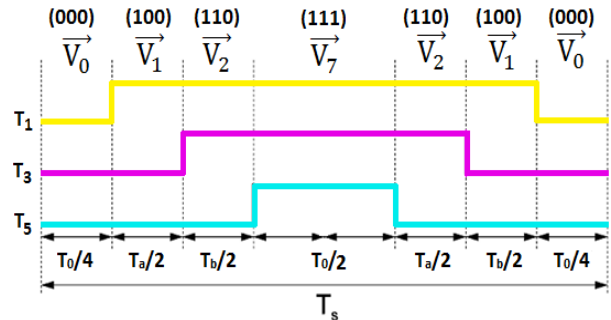


Fig. 7. The most suitable switching sequence for first section

### 4.1.4 Switching Signals

Total switching durations is collected by considering the most suitable switching sequence and reference control voltages ( $S_1, S_3, S_5$ ). There are 120 degrees phase differences between these reference voltages and their waveforms are similar to seagull. The algorithm needed to obtain the switching signals is shown in Fig. 8. Owing to this algorithm, the reference control voltages ( $S_1, S_3$  and  $S_5$ ) are obtained as shown in Fig. 9. Then, according

as principle of PWM, the reference control voltages obtained are compared with a carrier triangle wave. Consequently, the switching signals of semiconductor elements on the back to back converter are obtained. The comparison of reference control voltages and carrier triangle wave obtained is shown Fig. 9.

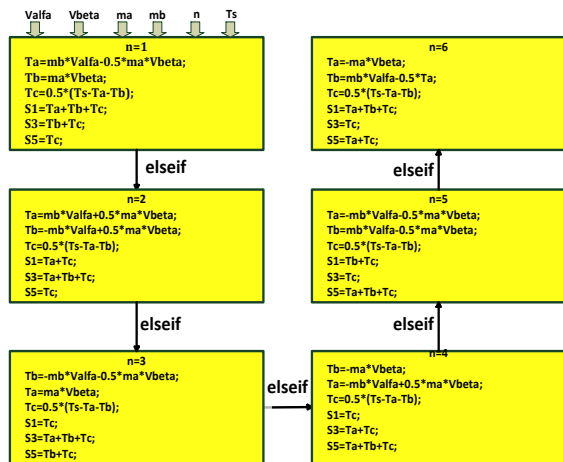


Fig. 8. The algorithm developed to obtain the switching signals

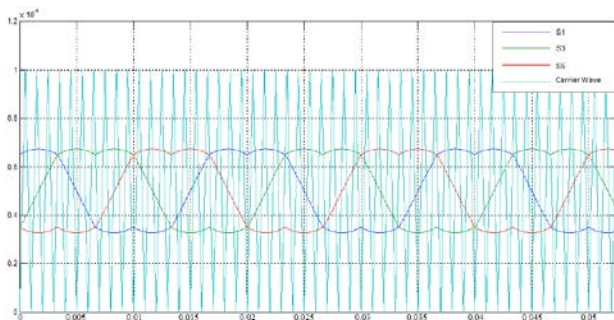


Fig. 9. Comparison of reference control voltages and carrier triangle wave

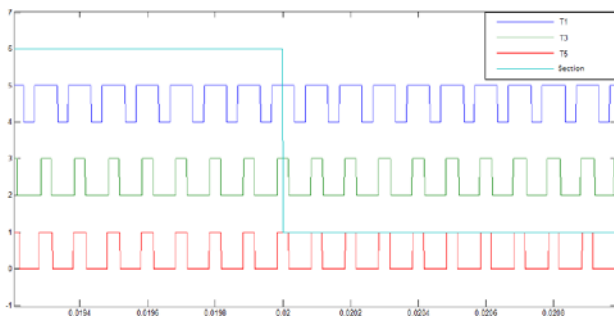


Fig. 10. The switching signals for sixth section and the first section

#### 4.2 Hysteresis Current Control (HCC)

Aim of this control is to keep outside the current of converter within a hysteresis band determined. HCC block diagram for one phase in MATLAB/Simulink is shown in Fig. 11.

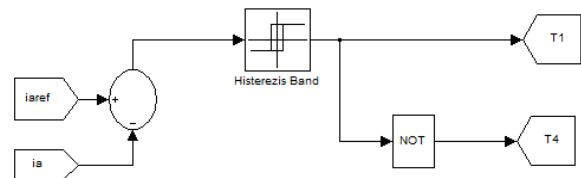


Fig. 11. HCC block diagram for one phase in MATLAB/Simulink

In here, the measured load currents are compared with the references by using hysteresis comparators. Each comparator determines the switching state of the corresponding inverter leg such that the load currents are forced to remain within the hysteresis band. Based on the band, there are two types of current controllers, namely, fixed band and sinusoidal band hysteresis current controller [10].

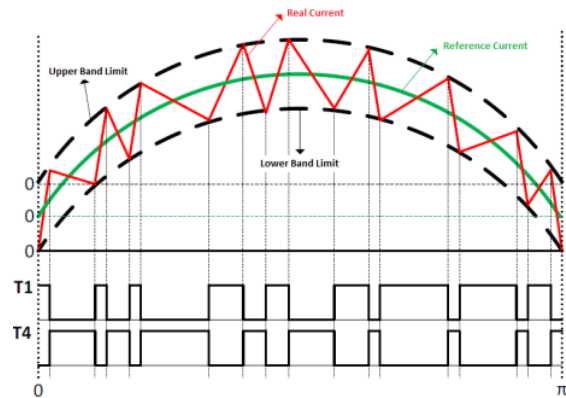


Fig. 12. HCC A phase current wave and the first phase arm IGBT control signal

Upper band and lower band limits for reference and real currents are determined by hysteresis band for a phase. As shown in Fig. 12, the ripple of real current always is within hysteresis band. If real current reaches or exceeds to upper band, while the element on upper of the first phase arm is turned off ( $T1=0$ ), the element on upper of

the first phase arm is turned on ( $T4=1$ ). Thus, the current is reduced. Conversely, if real current reaches or exceeds to lower band, while the element on upper of the first phase arm is turned on ( $T1=1$ ), the element on upper of the first phase arm is turned off ( $T4=0$ ). Thus, the current is increased.

This control technique's advantages:

- The simple control algorithm
- Dynamic response speed

There is no need to information about load parameters [11].

### 4.3 Sinusoidal PWM

The most popular PWM approach is the sinusoidal PWM. In this method, a triangular (carrier) wave is compared to a sinusoidal wave at the desired fundamental frequency. So, the relative levels of the two signals are used to determine the pulse widths and control the switching of devices in each phase leg of the inverter.

Therefore, the pulse width is a sinusoidal function of the angular position [8]. In SPWM technique, the generated reference voltages are continuously compared with the triangular carrier wave. When the value of the sine wave is greater than triangular wave, the upper switch of the related phase is switched ON; otherwise the lower switch is switched ON. Due to SPWM technique, the output contains less harmonic content as compared to the square wave inverter.

The output contains the high frequency harmonics which depends upon the frequency modulation index. As the frequency modulation index increases the harmonic spectrum shifts towards higher frequency, which can be easily filtered out. To be increased the index also leads to increase in switching frequency. The amplitude of output voltage can be controlled by varying the amplitude of the reference voltage [12].

## 5. SIMULATION RESULTS AND DISCUSSION

Comparison of SVPWM, SPWM and HCC control techniques used to obtain converter switch signals in speed control of PMSG are analyzed in terms of dynamic response, harmonic content, torque ripple and current ripple with MATLAB/Simulink. The motor parameters used in simulation are given Table I. In HCC, the band width is set to hold constant the switching frequency by 10 kHz.

**Table 2.** Pmsg Parameters

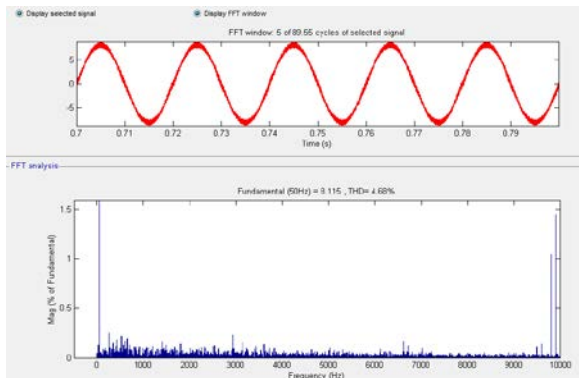
Nominal Power ( $P$ )	1.8 kW
Impedence ( $R_s$ )	0.775 $\Omega$
q-axis inductance ( $L_q$ )	7.31 mH
d-axis inductance ( $L_d$ )	7.31 mH
Magnetizing flux ( $\phi_m$ )	0.37387 Wb
Torque/Current ( $T/A$ )	1.1216 Nm/A
Pairs of poles ( $p_p$ )	2
Moment of Inertia ( $J$ )	0.00126811 kg/m <sup>2</sup>
Coefficient of Friction ( $B$ )	0

The analysis are carried out according to the values of  $V_{eff}= 155 V, f= 50 Hz$ , DC link capacitor voltage = 450 V and angular velocity of PMSG = 200 *rd/sec*. Additionally, the generator are applied to a load torque ( $T_e = 10 Nm$ ) depending on power obtained from wind. All of comparisons are made in the same conditionals as *PI* parameters, reference angular speed etc. The switching frequency is constant 10 kHz in SVPWM and SPWM but it is not constant in HCC. Because the ripple of current changes by depending on band width in HCC. Nevertheless, this three control technique based on a common value can be compared. Hence, in this paper, the setting band with is 0.852 values because it is provided that the average switching frequency is 10 kHz for HCC. It desired that the switching frequency varies nearly between 5 kHz - 15 kHz in fundamental cycle for 10 kHz average switching in HCC. This case can be determined by band with. The average switching frequency can be obtained by 10 kHz when band with is 0.852.

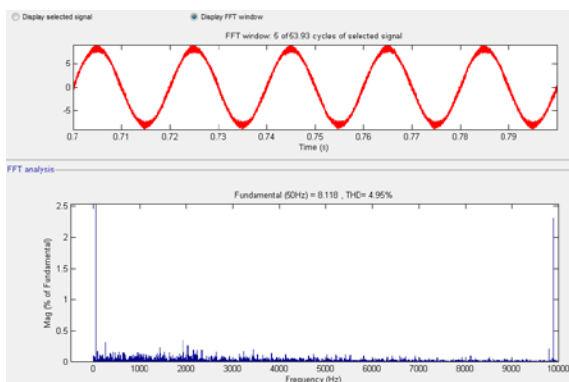
### 5.1 Comparison Based on THD

The current wave forms are usually discussed for

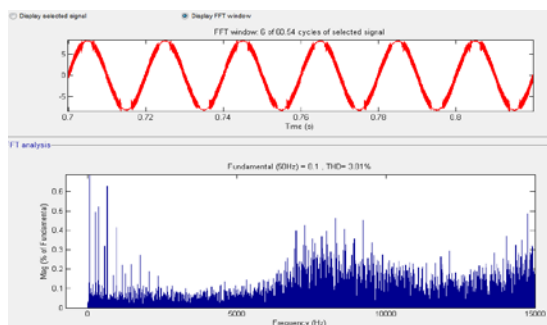
analysis of THD. In this paper, the integrity of system operation is provided and the grid current waveforms are examined for THD. Fig. 13 shows THD analysis at 10 kHz switching frequency for the grid currents with SVPWM, SPWM and HCC. THD values can read from Fig. 13.



(a)



(b)



(c)

**Fig. 13.** THD analysis for (a) SVPWM, (b) SPWM and (c) HCC techniques

As shown in Fig.13, THD of the grid currents obtained by using HCC is % 3.61; it is % 4.95 in SPWM and is %

4.68 in SVPWM. Therefore, HCC technique is more advantageous than the other two techniques in terms of current harmonic content. Besides, these results are quite suitable if it is considered that THD should be less than % 5 in inverter transferred to grid as mentioned in ref [11]. Similar results are observed for the currents of generator in a wind power system.

### 5.2 Comparison Based on Dynamic Response Speed

It is mentioned in ref [11] that dynamic response is required to be as fast as possible. The generator current waveforms obtained with SVPWM, SPWM and HCC by lowering the load torque at 0.6 seconds are showed in Fig. 14. In here, according to motor parameters, Torque/Current value is 1.12 Nm/A. Since torque is 10 Nm in this study, peak value of generator's current must be 8.9 A.

As shown in the Fig. 14, in such a case while real current becomes zero time 200 micro-seconds with SVPWM and SPWM technique, it becomes zero time about 70 micro-seconds. The reason of these results that SVPWM and SPWM control block has three PI controllers but HCC has one PI controller for both generator side control and grid side control. Therefore, it is clear that the use of HCC technique is better than the use of both SVPWM and SPWM in terms of dynamic response. Likewise, similar results are observed for the currents of grid in a wind power system.

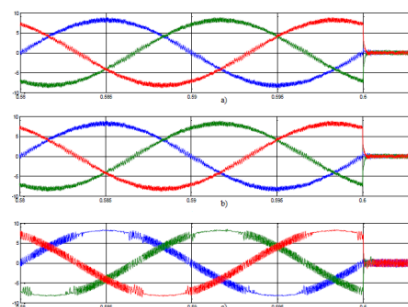


**Fig. 14.** Dynamic response analysis of the generator currents for (a) SVPWM, (b) SPWM and (c) HCC techniques

### 5.3 Comparison Based on Torque Ripple

The ripple is an undesirable situation in power systems. The ripple of electromagnetic torque obtained separately by using SVPWM, SPWM and HCC is shown on Fig.15. As results obtained, the torque ripple is about 1.33 in control with HCC and it is about 0.9 in control with SPWM while it is about 0.75 in control with SVPWM.

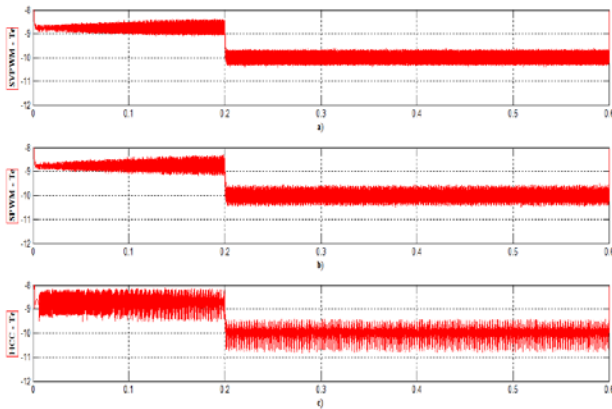


Fig. 15. Torque ripple analysis for (a) SVPWM, (b) SPWM and (c) HCC techniques

### 5.4 Comparison Based on the Grid Current Ripple

It can be examining to grid currents shown in Fig.16 for the current ripple quality between the use of SVPWM, SPWM and HCC techniques. As results obtained, the ripple is about 1.704 (2BW) in control with HCC and it is about 1.5 in control with SPWM while it is evaluated about 1.15 in control with SVPWM.

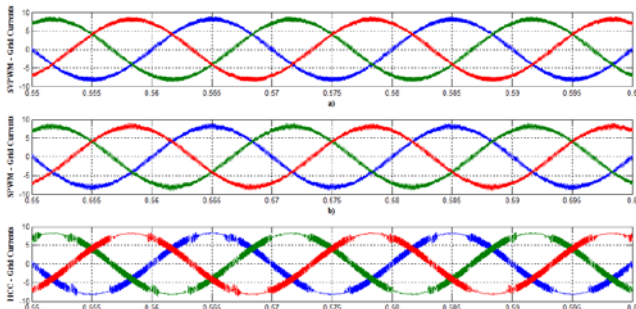


Fig. 16. The grid currents ripple analysis for (a) SVPWM, (b) SPWM and (c) HCC techniques

So, it is clear that the control with SVPWM is more suitable than control with HCC systems in terms of

ripple factor. Consequently, Table 3 is formed according as the results obtained.

Table 3. Comparison of Control Techniques

Type of Controller	Current THD	Dynamic Response	Torque Ripple	Current Ripple
SVPWM	% 4.68	Slower	Lower	Lower
SPWM	% 4.95	Slower	Medium	Medium
HCC	% 3.61	Faster	Higher	Higher

### 5.5 Comparison of SVPWM and SPWM Based on the Use of DC Link Voltage

In addition to those described results, the literature research says to have benefited % 15 more from the DC bus with SVPWM control technique compared with SPWM. Also, modulation index to obtain same output voltage is equal  $\sqrt{3} \cdot V_{ref} / V_{dc}$  in SVPWM while it is equal  $V_{dc} / 2$  in SPWM [13]. In this paper, this result also is obtained. Modulation index ( $m_a$ ) obtained with SVPWM while output voltage is equal to 155.88V is shown Fig. 17. In the same way,  $m_a$  obtained with SPWM while output voltage is equal to 155.88V is shown Fig. 18.

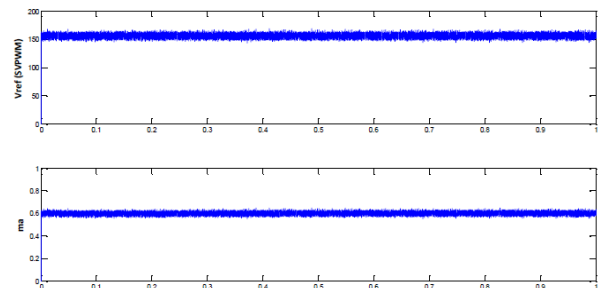


Fig. 17. Modulation index obtained with SVPWM for 155.88 V output voltage

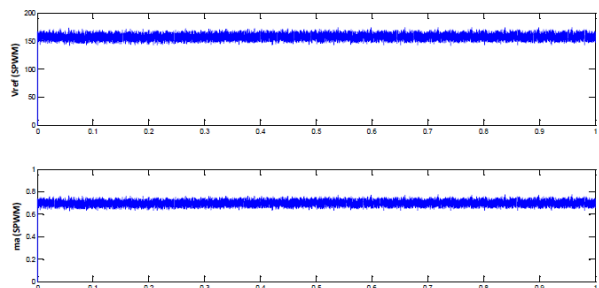


Fig. 18. Modulation index obtained with SPWM for 155.88 V output voltage

As shown in figures,  $m_a$  is 0.6 in SVPWM while  $m_a$  is 0.69 in SPWM in case of obtained the same output voltage. The rate of these modulation index is 15 percent. So, it is clear that it has benefited % 15 more from the DC bus with SVPWM control technique compared with SPWM.

In other words, it can be commented that these modulation index values in that if modulation indexes are equal for SVPWM and SPWM then it will be produced % 15 more output voltage in SVPWM than in SPWM.

## 7. CONCLUSIONS

In this paper, the performance of system is tested in MATLAB/Simulink by using SVPWM, SPWM and HCC in the control of SMSG. For this, PMSG is connected to grid via a back to back converter and power transfer to grid is provided. It is examined that modulation techniques (HCC, SPWM and SVPWM) used to be obtained switching signals of back to back converter and in terms of some features impact to system of these techniques is researched.

By considering all specifications by looking TABLE III and the other results, the use of SVPWM is more suitable than HCC and SPWM for speed control of PMSG. SVPWM uses lower DC link voltage for the given application and reduces the harmonic content of both grid current and generator current. Because of its superior performance characteristics, the space vector modulation technique is widely used in recent years.

## REFERENCES

- [1] A. Rolan, A. Luna, G. Vazquez, D. Aguliar, and G. Azevedo, "Modelling of a Variable Speed Wind Turbine with a Permanent Magnet Synchronous Generator," IEEE International Symposium on Industrial Electronics, Seoul, pp. 734-739, 2009
- [2] C. Busca, A.I. Stan, T. Stanciu D.I. Stroe, "Control of Permanent Magnet Synchronous Generator for Large Wind Turbines," Industrial Electronics Symposium, Bari 2010, pp. 3871-3876
- [3] M.M. Hussein, M. Orabi, M.E. Ahmed, M.A. Sayed, "Simple Sensorless Control Technique of Permanent Magnet Synchronous Generator Wind Turbine, International Conference on Power and Energy," Kuala Lumpur, Malaysia, 2010, pp. 512-517.
- [4] K. Huang, S. Huang, F. She, B. Luo, L. Cai, "A Control Strategy for Direct-drive Permanent Magnet Wind Power Generator Using Back to Back PWM Converter," ICEMS 2008 Conference, Wuhan, pp. 2283-2288.
- [5] S. Yang, L. Zhang, "Modelling and Control of the PMSG Wind Generation System with A Novel Controller," Third International Conference on Intelligent System Design and Engineering Applications, 2013, pp. 946-949
- [6] J. Pradeep, R. Devanathan, "Comparative Analysis and Simulation of PWM and SVPWM Inverter Fed Permanent Magnet Synchronous Motor," ICETEEEM Conference, 2012, India.
- [7] A. Cimpoer, "Encoderless Vector Control of PMSG for Wind Turbine Applications," Master Thesis, Aalborg University Institute of Energy Technology, 2010, Denmark.
- [8] E. Hendawi, F. Khater, A. Shaltout, "Analysis, Simulation and Implementation of Space Vector Pulse Width Modulation Inverter," 9th WSEAS International Conference
- [9] K.V. Kumar, P.A. Michael, J.P. John, S.S. Kumar, "Simulation and Comparison of SPWM and SVPWM Control for Three Phase Inverter," ARPN Journal of Engineering and Applied Sciences, pp. 63-74, 2010
- [10] A. Nachiappan, K. Sudararajan, V. Malarselvam, "Current Controlled Voltage Source Inverter Using Hysteresis Controller and PI Controller," EPSCICON Conference, 2012, Kerala.

- [11] E. İsen, A.F. Bakan, "Comparison of SVPWM and HCC Control Techniques in Grid Connected Three Phase Inverters," ELECO 2010, 264-268.
- [12] R. Bhosale, J. Shaikh, R. Bindu, "Analysis of Inverter Modulation Strategies for Vector Controlled Drives," International Journal of Advances in Electrical and Electronics Engineering, pp. 80-87
- [13] B. K. Swamy, P. N. Rao, "Simulation of A Space Vector PWM Controller for A Three-Level Voltage-Fed Inverter Motor Drive," International Journal of Advanced Trend in Computer Science and Engineering, 2013, pp. 363-372
- [14] H. Shariatpanah, R. Fadaeinedjad, G. Moschopoulos, "An investigation of furl control in a direct-drive PMSG Wind Turbine," Telecommunications Energy Conference, 2014, Vancouver Canada.
- [15] A. Kumar, B. Parasannakumari, E. Varghese, "Space Vector PWM and Fractional Controller based Wind Energy Conversion Systems," International Conference on Advances in Green Energy, 2014, Trivandrum.
- [16] M. R. Abedi, K. Y. Lee, "Modelling, Operation and Control of Wind Turbine with Direct Drive PMSG Connected to Power Grid," Pes General Meeting Conference, 2014.
- [17] J. Sabarad, G. H. Kulkarni, "Comparative Analysis of SVPWM and SPWM Techniques for Multilevel Inverter", International Conference on Power and Advanced Control Engineering, 2015, pp. 232-237.
- [18] N. Viswanath, A. K. Kapoor, "Performance Estimation of HCC and SVPWM Current Control Techniques on Shunt Active Power Filters", International Conference on Power,Control and Embedded Systems, 2010, pp 1-6